Kinetic Study on the UV-Induced Photopolymerization of Epoxy Acrylate/TiO_2 Nanocomposites by FTIR Spectroscopy

Fusheng Li, Shuxue Zhou, Bo You, Limin Wu

Department of Materials Science, The Advanced Coatings Research Center of China Educational Ministry, Fudan University, Shanghai 200433, People's Republic of China

Received 2 May 2005; accepted 8 July 2005
DOI 10.1002/app.22573
Published online in Wiley InterScience (www.interscience.wiley.com).

ABSTRACT: The kinetics of the photopolymerization of epoxy acrylate/TiO_2 nanocomposites, with 2′2-dimethoxy-1,2-diphenylethan-1-one (Irgacure 651) or benzophenone/*N*-methyl diethanolamine as photoinitiators, were studied by FTIR spectroscopy. It was found that nanocomposites had a decreasing photopolymerization rates in comparison with pure epoxy acrylate. The photopolymerization rate of the nanocomposite could also be influenced by initiator types, oxygen, film thickness, irradiation intensity, dispersing media of TiO_2 slurry, and so forth. © 2006 Wiley Periodicals, Inc. J Appl Polym Sci 99: 3281–3287, 2006

Key words: TiO_2; nanocomposite coatings; photopolymerization kinetics; UV curing

INTRODUCTION

Nanocomposite was a new kind of composite material with an ultrafine phase dispersed in 1–100 nm size, and showed very interesting properties dramatically different from the conventional ones.[1–4] Among them, nanocomposite with nanoscaled TiO_2 embedded has gained great interests of scientists and researchers around the world in the last decades because of its unique properties and good performance.[5–10]

Various polymer/TiO_2 nanocomposites were prepared by sol–gel process for different purposes and various applications, specifically, optical and electric functional nanocomposites had been the focus of recent study. For example, Yang[11,12] and coworkers and Zhang[13] et al. had successfully prepared PPV/TiO_2 nanocomposites with improved zero-phonon vibronic transition and increased vibronic splitting energy. Nussbaumer et al.[9] prepared a series of nanocomposites with high refractive index, incorporating the TiO_2 colloids into poly(vinyl alcohol), partially hydrolyzed poly(vinyl acetate), poly(vinyl pyssrrolidone), and poly(4-vinyl pyridine). Besides, nanocomposites of polypyrrole/TiO_2,[14] polyaniline/TiO_2,[15] poly(thiourethane)/TiO_2,[16] poly(styrene maleic anhydride)/TiO_2,[17] and polyether/TiO_2,[18] with improved optical properties or electrical properties, were reported as well. Solar cells, based on the nanocomposites of poly(3-hexylthiophene)/TiO_2[19] and polythiophene/TiO_2,[20] showed some excellent photovoltaic cell efficiency. Furthermore, the nanocomposites with TiO_2 embedded also showed some improved electrochemical property,[21] light-driven oxygen scavenging property,[22] gas-separation property,[23,24] photocatalytic property,[25–28] and electrorheological property.[29] Even when the TiO_2 was simply used as the filler for the coatings, plastics, and rubbers, the resultant nanocomposites showed improved performance in mechanic,[30] thermal,[31,32] UV-shielding,[33] dynamic fracture toughness,[34] ethanol permselectivity,[34] flame retardancy,[35] optical transparency,[36] scratch resistance,[37]chemical resistance,[38] and so forth.

Up to now, however, no report was focused on the kinetics of photopolymerization of UV-curable nanocomposites, containing nanoscaled TiO_2. Since nanoscaled TiO_2 could absorb UV rays by increasing the weatherability of polymers, we would believe that the nanoscaled TiO_2 should have some impact on the photopolymerization behavior of the UV-curable nanocomposite coatings with nanoscaled TiO_2.

EXPERIMENTAL

Materials

Rutile TiO_2 (50 nm) was supplied by the Kemira Chemical Company (Pori, Finland). *N*-butyl acetate

Correspondence to: L. Wu (lxw@fudan.ac.cn).
Contract grant sponsors: Shanghai Special Nano Foundation; The Doctoral Foundation of University; Trans-century Outstanding Talented Person Foundation of China Educational Ministry; and Key Project of China Educational Ministry.

TABLE I
The Formulations for Preparation of EA/TiO_2 Nanocomposite Coatings

Sample code	EA	HDDA	TSB	TST	TMPTA	Irgacure 651	BP	MDEA
Pure-I3					16	1.2		
TST1-I3				4	12	1.2		
TST2-I3				8	8	1.2		
TST3-I3				12	4	1.2		
TST4-I3				16		1.2		
TSB1-I3			4		15.6	1.2		
TSB2-I3	16	8	8		15.2	1.2		
TSB3-I3			12		14.8	1.2		
TSB4-I3			16		14.4	1.2		
PURE-BM3					16		0.72	0.48
TSB1-BM3			4		15.6		0.72	0.48
TSB4-BM3			16		14.4		0.72	0.48
TST1-BM3				4	12		0.72	0.48
TST4-BM3				16			0.72	0.48

(AP) was purchased from the Shanghai Chemistry Reagent Co. Ltd (China). 2,2-dimethoxy-1,2-diphenylethan-1-one (Irgacure 651) was a gift of Ciba Specialty Chemicals. *N*-methyl diethanolamine (MDEA) and benzophenone (BP) were provided by Changzhou Wujin No. 5 Chemical Factory (Changzhou, China). Trimethylolpropane triacrylate (TMPTA) and 1,6-hexanediol diacrylate(HDDA)were purchased from Eternal Chemical company (Taiwan, China). Epoxy acrylate (EA oligomers, M_w 1000) was the product of Sanmu Corp. (Yixing, China). All these materials were used as received.

Preparation TiO_2 slurry and EA/TiO_2 nanocomposites

Preparation TiO_2 slurry

TiO_2 with TMPTA or butyl acetate as the media was milled by minizeta milling machine (Netzsch machinery and instruments Co. Ltd., Germany), with the grinding speed of 2600 rpm and 0.6–0.8 mm ZrO_2 beads, for 2 h to obtain 10 wt % TiO_2 slurry for further use. The TiO_2 slurry with TMPTA or butyl acetate as the media was designated as TST or TSB, respectively.

The preparation of EA/TiO_2 nanocomposites

The TST or TSB was added into TMPTA and HDDA, and treated with ultrasonication for 30 min, and then added into EA oligomeric resin and ultrasonicated for another 30 min, followed by addition of photoinitiator. Table I listed the formulations. The sample codes TSTa-Bi or TSBa-Bi indicated the nanocomposites embedded with TST or TSB, respectively, *a* represent nanoscaled TiO_2 solid percent, based on the weight of the total system, but initiator *B* denoted by *I* or BM for photoinitiators Irgacure 651 or BP/MDEA, respectively, and *I* indicated the weight percent, based on the weight of the total system.

UV-curing kinetics of nanocomposites

The FTIR spectra of samples before curing and after different UV-curing time were scanned by a Magna-IR^{TM} 550 spectrometer (Nicolet Instruments, Madison, WI). In this study, the sandwich-like NaCl plates were used for the FTIR scanning, to minimize the influence of oxygen in the atmosphere. Unless otherwise noted, all the samples were investigated in the laminate state (sandwich-like), and the thickness of nanocomposites was about 20 μm.

RESULTS AND DISCUSSION

Preparation of TiO_2 slurry and corresponding nanocomposites

The TiO_2 particles, with an average diameter of 50 nm, were used to prepare the TiO_2 slurry, with butyl acetate or TMPTA as the media. After 2-h milling, the TiO_2 particles were successfully dispersed into both butyl acetate and TMPTA, at the mean diameter of 50–60 nm, as indicated in Figure 1. Both TiO_2 slurries had a very good stability, and no phase separation was observed after 4-week's storage.

After introducing the prepared TiO_2 slurry into the EA resin, a series of nanocomposites were prepared. Figure 2 showed the viscosity of nanocomposite coatings as a function of TiO_2 content. It could be seen that the viscosity of the nanocomposite coating increased with increasing TST, but decreased with increasing TSB, indicating that TMPTA increased the viscosity of UV-curable nanocomposite, while butyl acetate could decrease the viscosity.

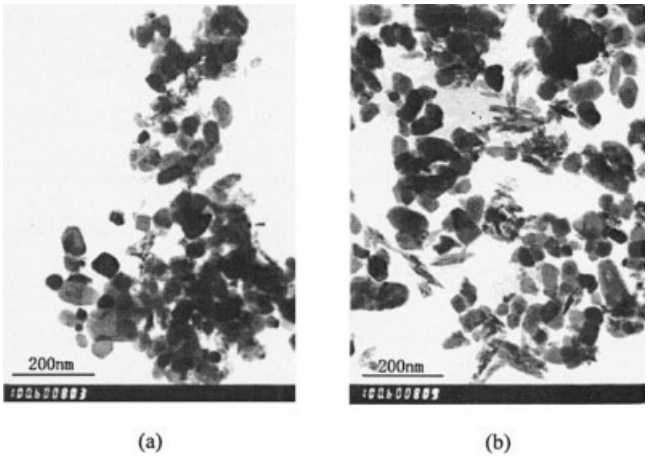

Figure 1 TEM photos for the TiO_2 slurry with (a) TMPTA and (b) butyl acetate as the media.

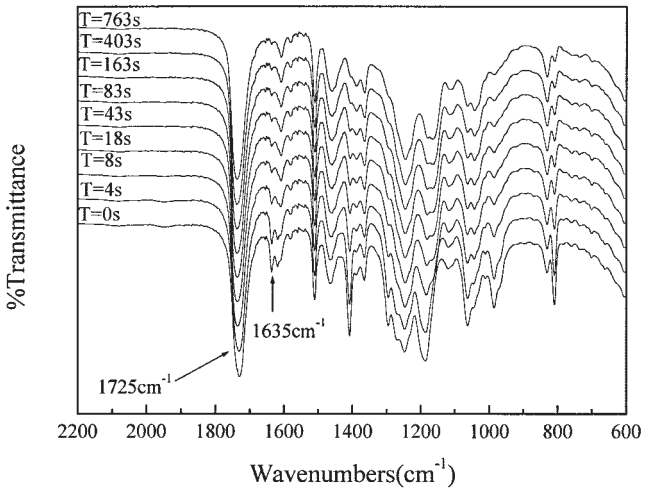

Figure 3 The FTIR spectra of UV-nanocomposite coatings, at different irradiation times (2.1 mW/cm^2, 3 wt % Irgacure 651).

Typical photopolymerization kinetics of nanocomposites

The typical FTIR spectra of UV-curable nanocomposite coatings, with different irradiation time, were shown in Figure 3. It was found that the intensity of the peak at 1635 cm^{-1} for C═C stretching absorbance decreased with increasing exposure time under UV irradiation, since the peak at 1635 cm^{-1} was well separated from other peaks. It was usually used to quantify the conversion of C═C bond in UV-curable coatings, with the peak at 1725 cm^{-1} due to C═O stretching absorbance as the reference, for its invariability during UV curing.[39,40] Thus, the conversion percent (C) of C═C bond could be calculated, according to the following equation:

$$C(\%) = 100 \times \left(1 - \frac{A_t S_0}{A_0 S_t}\right) \quad (1)$$

where A_t and A_0 were the areas of the peak at 1635 cm^{-1} and S_t and S_0 the areas of the peak at 1725cm^{-1} at time t and $t = 0$, respectively.

Based on the data calculated by eq. (1), the conversion curve for the UV-curable nanocomposite coatings, containing 4 wt % nanoscaled TiO_2 as a function of curing time, was plotted in Figure 4. The curve for the pure EA photopolymerization was also presented for the sake of comparison. The induction time for nanocomposites at the beginning of photopolymerization was negligible. Then, an acceleration of the polymerization rate was observed because of the gel effect. After that, the polymerization rate slowed down because of the vitrification of the resin. This was consistent with the typical kinetic curve of the UV-curable coatings with three functionality reactive dilutes.[41]

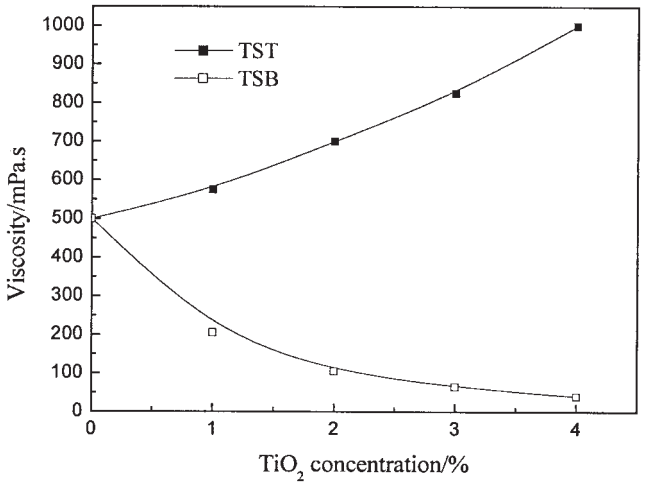

Figure 2 The viscosity curve of nanocomposites containing TST and TSB.

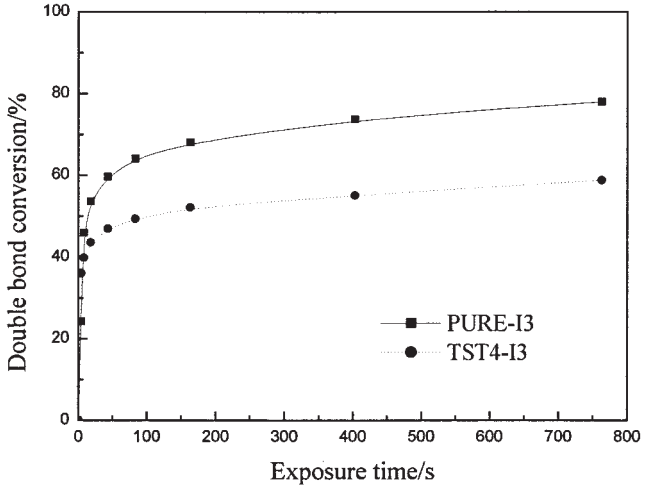

Figure 4 The plot of photopolymerization kinetics of nanocomposites (3 wt % Irgacure 651, 2.1 mW/cm^2 at 365 nm).

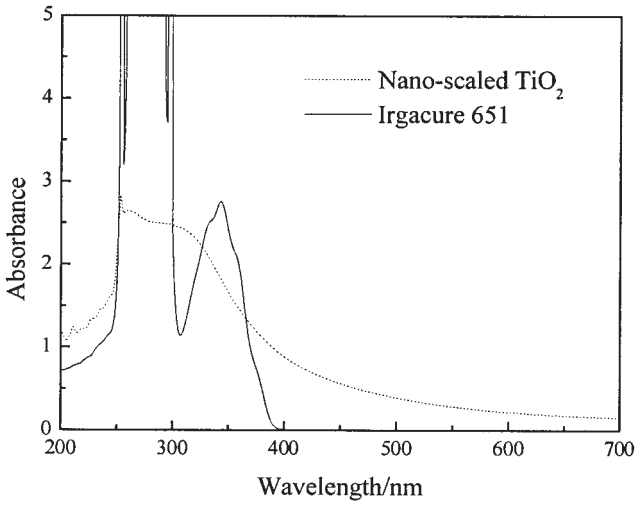

Figure 5 UV–vis spectra for Irgacure 651 and nanoscaled TiO_2.

The nanocomposites had a decreasing photopolymerization rate compared with pure EA, which was different from the kinetics of the nanocomposites embedded with nanoscaled SiO_2.[42] This should be attributed to the strong adsorption of nanoscaled TiO_2 in the same UV-sensitive range as the photoinitiator, Irgacure 651, as shown in Figure 5, decreasing the initiating efficiency of Irgacure 651.

Effect of the photoinitiator type

The effects of the photoinitiator types on the photopolymerization kinetics of the nanocomposite coatings were displayed in Figure 6. The nanocomposite coatings with Irgacure 651 as the photoinitiator had faster photopolymerization and shorter induction time, than those initiated by BP/MDEA. This can be easily understood, based on their distinctive initiating mechanisms: the Irgacure 651 is Norrish type I photoinitiator, which undergoes a direct photofragmentation process (α- or less common β-cleavage).[43] Under the UV radiation, 2 moles of primary radicals can be obtained from 1 mole of Irgacure 651(see Fig. 7). Those 2 moles of primary radicals can react with the monomers and dissolve in oxygen. So, the oxygen dissolved in the formulation can be consumed instantly. But for the BP/MDEA initiating system, it is not so efficient as Irgacure 651, since it belongs to the Norrish type II photoinitiator, involving a primary process of hydrogen atom abstraction from the MDEA (tertiary amine).[43] Only 1 mole of primary radical can react with the monomer, though there were 2 moles of primary radicals formed (see Fig. 7). As a result, an observable induction time was observed for the BP/MDEA initiating system, especially for sample TST4-BM3.

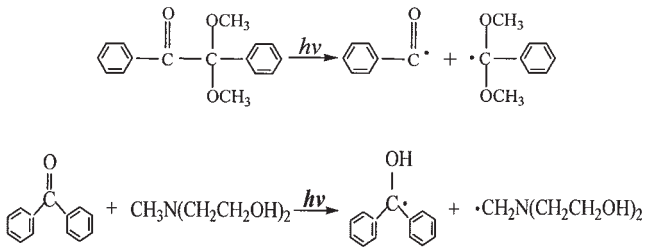

Figure 7 Photolysis of Irgacure 651 and BP/MDEA.

Effect of the TiO_2 content

Figure 8 showed the effect of nanoscaled TiO_2 content on the double bond conversion of nanocomposites with curing time. As the nanoscaled TiO_2 content in-

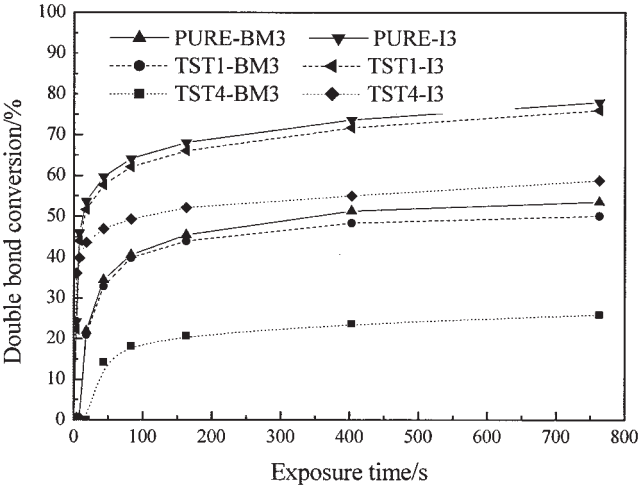

Figure 6 Influence of photoinitiator type on photopolymerization kinetics (3 wt % photoinitiators, 2.1 mW/cm^2 at 365 nm).

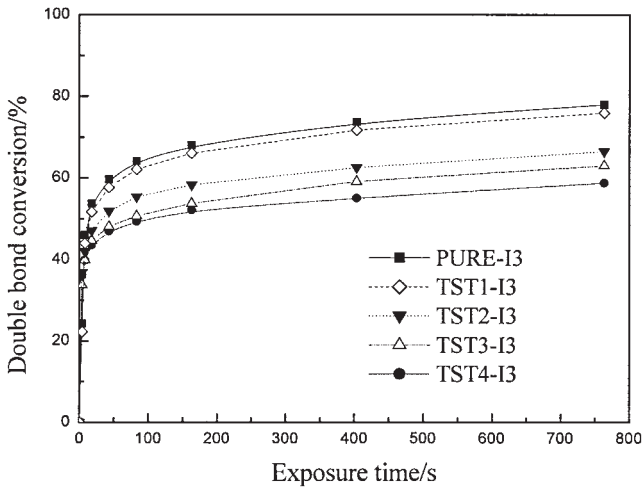

Figure 8 Influence of nanoscaled TiO_2 content on photopolymerization kinetics (3 wt % Irgacure 651, 2.1 mW/cm^2 at 365 nm).

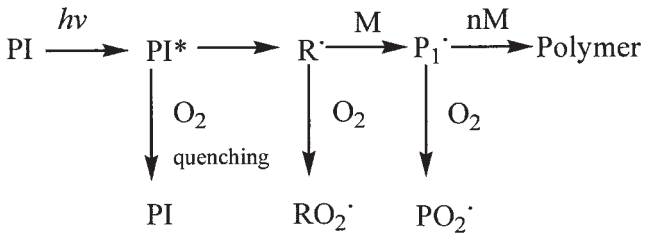

Figure 9 The oxygen inhibition in a radical-type photoinitiated polymerization.

creased, the curing rate and final double bond conversion decelerated monotonously. This was theoretically reasonable, since nanoscaled TiO_2 absorbed UV rays strongly in the range of 200–400 nm, decreasing the initiation efficiency of photoinitiator, just discussed earlier.

Effect of oxygen

The triplet states of photoinitiators and radicals formed from photoinitiators were strongly attacked by oxygen, leading to quenching and formation of peroxy radicals, respectively. The detrimental effect of oxygen on radical photopolymerization reactions was well known from the curing process performed with photoinitiators.[44,45] Specifically, the oxygen inhibition effect was realized mainly by quenching the triplet state photoinitiator, primary radicals, and polymer radicals,[44] as indicated in Figure 9.

A simple means to investigate the influence of molecular oxygen on photopolymerization of nanocomposites was to compare the kinetics in aerated and laminated systems. Figure 10 demonstrated the photopolymerization kinetics of pristine EA and nanocomposites containing 4 wt % nanoscaled TiO_2 in the air and laminate state. It could be seen that the nanocomposites had a lower curing rate both in air state and laminate state than pristine EA, and the existence of oxygen decelerated the photopolymerization of both pure EA and nanocomposite greatly. The decreasing difference in curing rate between the nanocomposite and pure EA resin in air state, in comparison with that in laminated state, suggests that the oxygen has lower inhibition effect on the photopolymerization of nanocomposite than that of pure EA resin. The possible reason was that the higher viscosity for nanocomposites made it less sensitive to the oxygen compared with the pure EA system.

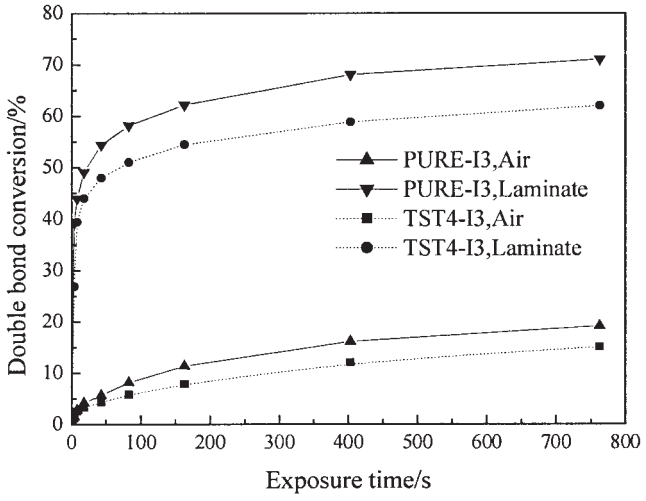

Figure 10 Photopolymerization kinetics in air state and laminate state (3 wt % Irgacure 651, 2.1 mW/cm^2 at 365 nm).

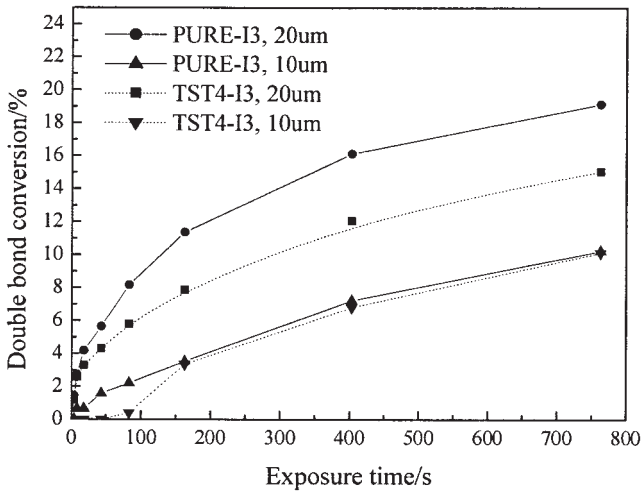

Figure 11 Effect of film thickness on photopolymerization kinetics in the presence of oxygen (3 wt % Irgacure 651, 2.1 mW/cm^2 at 365 nm).

Effect of film thickness

Another critical factor influencing the inhibition effect of oxygen was film thickness. Figure 11 presented the influence of film thickness on the photopolymerization kinetics. The double bond conversion of nanocomposites decreased with decreasing film thickness. The double bond conversion of 20-mm thick pure EA after 750 s UV irradiation was twofold of that in 10-mm thick pure EA, while 20-mm thick nanocomposite had around 1.4 times of 10-mm thick nanocomposite, further confirming that the oxygen had a decreasing inhibition effect on photopolymerization of nanocomposites in comparison with pure EA resin.

Effect of light intensity

Figure 12 illustrated the plots of photopolymerization for pure EA and nanocomposites under different irradiation intensity in laminate state and air state. Both photopolymerization rate and final double bond conversion increased as light intensity increased, for both

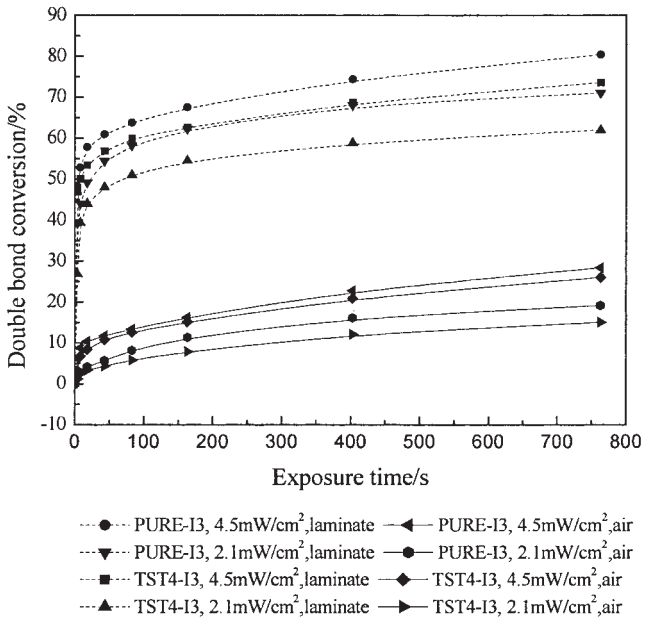

Figure 12 Effect of UV-radiation intensity on photopolymerization kinetics of nanocomposites in laminate state and in air state (3 wt % Irgacure 651, at 365 nm).

pristine EA and nanocomposites in air and laminated states. This increase can be explained by the following photopolymerization theory[46]:

$$\frac{d[R\cdot]}{dt} = 4.6\Phi I_0 \varepsilon [M]\frac{LA}{V} \qquad (2)$$

where $R'\cdot$ is the initiating radical; t the time; I_0 the number of Einsteins per cm^2 incident on the system per second; Φ the fraction f of the light quanta absorbed that resulted in the formation of a pair of radicals; ε the extinction coefficient; $[M]$ the monomer concentration in mol/L; and the geometric factor (LA/V) is unity, or nearly so, for most photolytic systems employed.

From eq. (2), $R'\cdot$ should be proportional to I_0. However, only the increasing tendency of $R'\cdot$ can be guaranteed with the increase of irradiation intensity because of the inhibition of oxygen in this case. Therefore, the double bond conversion was improved with the increasing irradiation intensity to various degrees.

The greater the light intensity the smaller the difference in photopolymerization rate between the nanocomposite and pure EA, no matter whether the oxygen was there or not. This suggested that increasing irradiation intensity can diminish or even eliminate the negative influence of nanoscaled TiO_2 on photopolymerization rates of nanocomposites.

Effect of different TiO_2 slurry

Heretofore, all the aforementioned studies on the photopolymerization kinetics of the nanocomposites was based on introducing the TST slurry into UV-curable systems; herein, we further investigated the effect of the TiO_2 slurry using butyl acetate (TSB) on the photopolymerization behavior of nanocomposites, since TiO_2 slurry was usually available, in some volatile solvent, as the dispersion media.

Figure 13 showed the photopolymerization kinetic curves of nanocomposites with different TSB content. It was very interesting that TSB obviously increased the photopolymerization rates of nanocomposites, and the photopolymerization rate increased with increasing TSB content, which was different from the effect of TST. Recall that introducing TST decreased the photopolymerization rate, since nanoscaled TiO_2 strongly absorbed UV rays and impaired the initiating efficiency of photoinitiator. The intuitionistic comparison shown in Figure 14, further confirmed that TSB had a rightabout impact on photopolymerization rate in comparison with TST. The reason why TSB could increase the photopolymerization rate was possibly because butyl acetate could enhance the mobility of the UV-curable system greatly, which preponderate over the negative effect of nanoscaled TiO_2 absorbing UV rays.

CONCLUSIONS

Nanoscaled TiO_2 could be used as UV absorber in plastics, coatings, inks, cosmetics, and other organic compounds, increasing the weatherability of these organic materials. But it was found that nanoscaled TiO_2 obviously decreased the photopolymerization rates of UV-curable systems, since nanoscaled TiO_2 could strongly absorb UV rays, decreasing the initiating efficiency of photoinitiator, based on this study. Therefore, in nanoTiO_2 contained UV-curable coatings, e.g.,

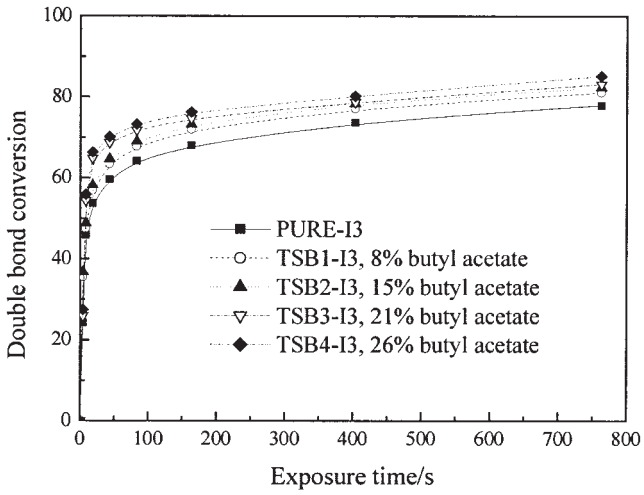

Figure 13 The influence of butyl acetate on the photopolymerization kinetics (3 wt % Irgacure 651, 2.1 mW/cm^2 at 365 nm).

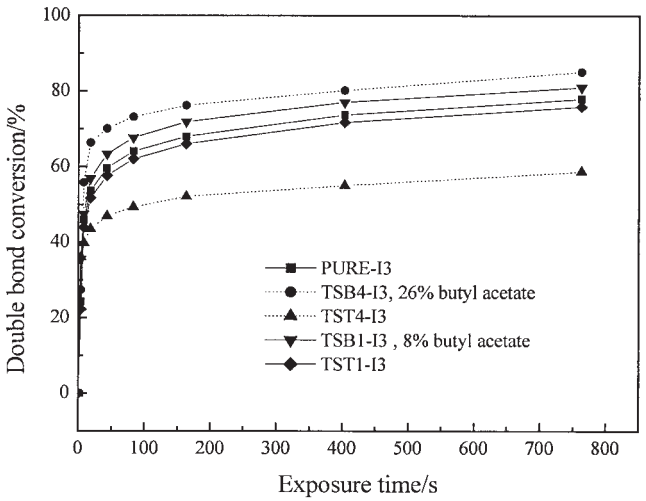

Figure 14 The influence of butyl acetate on the photopolymerization kinetics under 1 and 4% nanoscaled TiO_2 loading (3 wt % Irgacure 651, 2.1 mW/cm^2 at 365 nm).

one could tune the photopolymerization rates of the nanocomposites by adjusting initiator types, aerated or laminated state, film thickness, irradiation intensity, dispersing media of TiO_2 slurry, and so forth.

References

1. Hwang, D.; Moon, J.; Shul, Y.; Jung, K.; Kim, D.; Lee, D. J Sol-Gel Sci Technol 2003, 26, 783.
2. Valdez, M. T.; Jenouvrier, P.; Fick, J.; Paillard, E.; Langlet, M. Opt Mater 2004, 25, 179.
3. Wouters, M. E. L.; Wolfs, D. P.; Linde, M. C.; Hovens, J. H. P.; Tinnemans, A. H. A. Prog Org Coat 2004, 51, 312.
4. Wu, C. J Polym Sci Part A: Polym Chem 2005, 43, 1690.
5. Segawa, H.; Tateishi, K.; Arai, Y.; Yoshida, K.; Kaji, H. Thin Solid Films 2004, 466, 48.
6. Hiroi, R.; Ray, S. S.; Okamoto, M.; Shiroi, T. Macromol Rapid Commun 2004, 25, 1359.
7. Singh, R. S.; Grimes, C. A.; Dickey, E. C. Mat Res Innov 2002, 5, 178.
8. Imai, H.; Hirashima, H.; Awazu, K. Thin Solid Films 1999, 351, 91.
9. Nussbaumer, R. J.; Caseri, W. R.; Smith, P.; Tervoort, T. Macromol Mater Eng 2003, 288, 44.
10. Soucek, M. D.; Johnson, A. H.; Meemken, L. E.; Wegner, J. M. Polym Adv Technol 2005, 16, 257.
11. Yang, B.; Yoon, K. Synth Metal 2004, 142, 21.
12. Yang, B.; Yoon, K.; Chung, K. Mater Chem Phys 2004, 83, 334.
13. Zhang, J.; Ju, X.; Wang, B.; Li, Q.; Liu, T.; Hu, T. Synth Metal 2001, 118, 181.
14. Sharma Shailendra Sharma, G. D. J Mater Sci 2004, 15, 69.
15. Su, S.; Kuramoto, N. Synth Metal 2000, 114, 147.
16. Lu, C.; Cui, Z.; Guan, C.; Guan, J.; Yang, B; Shen, J. Macromol Mater Eng 2003, 288, 717.
17. Wang, S.; Zhang, L.; Su, H.; Zhang, Z.; Li, G.; Meng, G.; Zhang, J.; Wang, Y.; Fan, J.; Gao, T. Phys Lett A 2001, 281, 59.
18. Best, A. S.; Ferry, A.; MacFarlane, D. R.; Forsyth, M. Solid State Ionics 1999, 126, 269.
19. Kwong, C.; Djurisic, A.; Chui, P.; Cheng, K.; Chan, W. Chem Phys Lett 2004, 384, 372.
20. Roberson, L. B.; Poggi, M. A.; Kowalik, J.; Smestad, G. P.; Bottomley, L. A.; Tolbert, L. M. Coord Chem Rev 2004 248, 1491.
21. Hebestreit, N.; Hofmann, J.; Rammelt, U.; Plieth, W. Electrochim Acta 2003, 48, 1779.
22. Li, X.; Green, A. N. M.; Haque, S. A.; Mills, A.; Durrant, J. R. J Photochem Photobiol Chem 2004, 162, 253.
23. Kong, Y.; Du, H.; Yang, J.; Shi, D.; Wang, Y.; Zhang, Y.; Xin, W. Desalination 2002, 146, 49.
24. Zoppi, R. A.; Neves, S.; Nunes, S. P. Polymer 2000, 41, 5461.
25. Kemmitt, T.; Al-Salim, N. I.; Waterland, M.; Kennedy, V. J.; Markwitz, A. Curr Appl Phys 2004, 4, 189.
26. Zan, L.; Tian, L.; Liu, Z.; Peng, Z. Appl Catal A 2004, 264, 237.
27. Wu, J.; Uchida, S.; Fujishiro, Y.; Yin, S.; Sato, T. Int J Inorg Mater 1999, 1, 253.
28. Yin, S.; Maeda, D.; Ishitsuka, M.; Wu, J.; Sato, T. Solid State Ionics 2002, 151, 377.
29. Zhao, X.; Duan, X. Mater Lett 2002, 54, 348.
30. Xiong, M.; You, B.; Zhou, S.; Wu, L. Polymer 2004, 45, 2967.
31. Xiong, M.; Zhou, S.; You, B.; Wu, L. J Polym Sci Part B: Polym Phys 2005, 43, 637.
32. Xiong, M.; Zhou, S.; You, B.; Gu, G.; Wu, L. J Polym Sci Part B: Polym Phys 2004, 42, 3682.
33. Xiong, M.; Zhou, S.; Wu, L.; Wang, B.; Yang, L. Polymer 2004, 45, 8127.
34. Evora, V. M. F.; Ahukla, A. Mater Sci Eng A 2003, 361, 358.
35. Zhang, J.; Wang, X.; Lu, L.; Li, D.; Yang, X. J Appl Polym Sci 2003, 87, 381.
36. Tong, Y.; Li, Y.; Xie, F.; Ding, M. Polym Int 2000, 49, 1543.
37. Ng, C. B.; Schadler, L. S.; Siegel, R. W. Nanostruct Mater 1999, 12, 507.
38. Nakane, K.; Kurita, T.; Ogihara, T.; Ogata, N. Compos B 2004, 35, 219.
39. Wang, J. Z.Y.; Bogner, R. H. Int J Pharm 1995, 113, 113.
40. Li, F.; Zhou, S.; Gu, G.; You, B.; Wu, L. J Appl Polym Sci 2005, 96, 912.
41. Decker, C. Polym Int 1998, 45, 133.
42. Li, F.; Zhou, S.; You, B.; Wu, L. J Appl Polym Sci 2005, to appear.
43. Norman, S. A. J Photochem Photobiol Chem 1996, 100, 101.
44. Studer, K.; Decker, C.; Beck, E.; Schwalm, R. Prog Org Coat 2003, 48, 101.
45. Studer, K.; Decker, C.; Beck, E.; Schwalm, R. Prog Org Coat 2003, 48, 92.
46. Allcock, H. R.; Lampe, F. W.; Mark, J. E. Contemporary Polymer Chemistry; Science Publisher: Beijing, China, 2004; p 120.